

## On multidimensional data and modern disks

Steven W. Schlosser<sup>†</sup>, Jiri Schindler<sup>‡</sup>, Stratos Papadomanolakis<sup>\*</sup>, Minglong Shao<sup>\*</sup>,  
Anastassia Ailamaki<sup>\*</sup>, Christos Faloutsos<sup>\*</sup>, Gregory R. Ganger<sup>\*</sup>  
<sup>†</sup>Intel Research Pittsburgh, <sup>‡</sup>EMC Corporation, <sup>\*</sup>Carnegie Mellon University

### Abstract

With the deeply-ingrained notion that disks can efficiently access only one dimensional data, current approaches for mapping multidimensional data to disk blocks either allow efficient accesses in only one dimension, trading off the efficiency of accesses in other dimensions, or equally penalize access to all dimensions. Yet, existing technology and functions readily available inside disk firmware can identify non-contiguous logical blocks that preserve spatial locality of multidimensional datasets. These blocks, which span on the order of a hundred adjacent tracks, can be accessed with minimal positioning cost. This paper details these technologies, analyzes their trends, and shows how they can be exposed to applications while maintaining existing abstractions. The described approach can achieve the best possible access efficiency afforded by the disk technologies: sequential access along primary dimension and access with minimal positioning cost for all other dimensions. Experimental evaluation of a prototype implementation demonstrates a reduction of overall I/O time for multidimensional data queries between 30% and 50% when compared to existing approaches.

### 1 Introduction

Large, multidimensional datasets are becoming more prevalent in both scientific and business computing. Applications, such as earthquake simulation and oil and gas exploration, utilize large three-dimensional datasets representing the composition of the earth. Simulation and visualization transform these datasets into four dimensions, adding time as a component of the data. Conventional two-dimensional relational databases can be represented as multidimensional data using online analytical processing (OLAP) techniques, allowing complex queries for data mining. Queries on this data are often ad-hoc, making it difficult to optimize for a particular workload or access pattern. As these datasets grow in size and popularity, the performance of the applications that access them growing in importance.

Unfortunately, storage performance for this type of data is often inadequate, largely due to the one-dimensional abstraction of disk drives and disk arrays. Today's data placement techniques are commonly predicated on the assumption that multidimensional data must

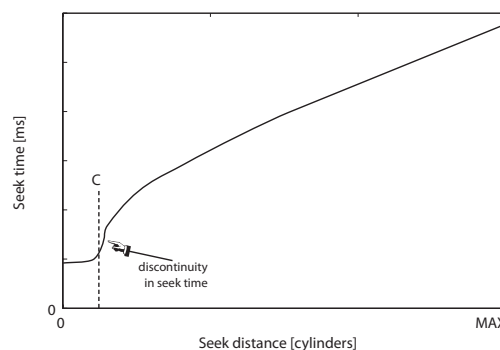


Figure 1: **Notional seek curve of a modern disk drive.** The seek time profile of a modern disk drive consists of three distinct regions. For cylinder distances less than  $C$ , the seek time is constant, followed by a discontinuity. After this point of discontinuity, the seek time is approximately the square root of the seek distance. For distances larger than one third of the full seek distance, the seek time is a linear function of seek distance. To illustrate the trend more clearly, the X axis is not drawn to scale.

be serialized when stored on disk. Put another way, the assumption is that spatial locality cannot be preserved along all dimensions of the dataset once it is stored on disk. Various data placement and indexing techniques have been proposed over the years to optimize access performance for various data types and query workloads, but none solve the fundamental problem of preserving locality of multidimensional data.

Some recent work has begun to chip away at this assumption [13, 27], showing that locality in two-dimensional relational databases can be preserved on disk drives, but we believe that these studies have only scratched the surface of what is possible given the characteristics and trends of modern disks. In this paper, we show that modern disk drives *can* physically preserve spatial locality for multidimensional data. Our technique takes advantage of the dramatically higher densities of modern disks, which have increased the number of tracks that can be accessed within the time that it takes the disk head to settle on a destination track. Any of the tracks that can be reached within the settle time can be accessed for approximately equal cost, which contrasts with the standard “rule of thumb” of disk drive technology that longer seek distances correspond to longer seek times.

Figure 1 illustrates the basic concept using a canonical seek curve of a modern disk drive. In contrast to conven-

tional wisdom, seek time for small distances (i.e., fewer than  $C$  cylinders, as illustrated in the figure) is often a constant time equal to the time for the disk head to settle on the destination cylinder. We have found that  $C$  is not trivially small, but can be as high as 100 cylinders in modern disks. This means that on the order of 100 disk blocks can be accessed for equal cost from a given starting block. We refer to these blocks as being *adjacent* to the starting block, meaning that any of them can be accessed for equal cost.

In this paper, we explain the adjacency mechanism, detailing the parameter trends that enable it today and will continue to enable it into the future. We describe the design and implementation of a prototype disk array logical volume manager that allows applications to identify and access adjacent disk blocks, while hiding extraneous disk-specific details so as to not burden the programmer. As an example, we also evaluate a data placement technique that maps a three- and four-dimensional dataset onto the logical volume, preserving physical locality directly on disk, and improving spatial query performance by between 30% and 50% over existing data placements.

The rest of this paper is organized as follows. Section 2 describes related work. Section 3 describes details of the adjacency mechanism, how it can be implemented in modern disks, and historic and projected disk parameter trends that enable the adjacency mechanism. Section 4 analyzes data obtained from measurements of several state-of-the-art enterprise-class SCSI disks to show how their characteristics affect the properties of the adjacency mechanism. Section 5 shows how adjacency can be expressed to applications without burdening them with disk-specific parameters. Section 6 evaluates the efficiency of adjacent access on a prototype system using microbenchmarks as well as 3D and 4D spatial queries.

## 2 Background and related work

Effective multidimensional data layout techniques are crucial for the performance of a wide range of scientific and commercial applications. We now describe the applications that will benefit from our approach and show that existing techniques do not address the problem of preserving the locality of multidimensional data accesses.

### 2.1 Multidimensional datasets

Advances in computer hardware and instrumentation allow high-resolution experiments and simulations that improve our understanding of complex physical phenomena, from high-energy particle interactions to combustion and earthquake propagation. The datasets involved in modern scientific practice are massive and multidimensional. Modern simulations produce data at the staggering rate of multiple terabytes per day [21],

while high energy collision experiments at CERN are expected to generate raw data of a petabyte scale [33]. Realizing the big benefits of the emerging data-driven scientific paradigm heavily depends on our ability to efficiently process these large-scale datasets.

Simulation applications are a great example for the storage and data management challenges posed by large-scale scientific datasets. Earthquake simulations [2] compute the propagation of an earthquake wave over time, given the geological properties of a ground region and the initial conditions. The problem is discretized by sampling the ground at a collection of points and the earthquake’s duration as a set of time-steps. The simulator then computes physical parameters (like ground velocity) for each discrete ground point and for each time step. Post-processing and visualization applications extract useful information from the output.

The difficulties in efficiently processing simulation output datasets lie in their volume and their multidimensional nature. Storing one time-step of output requires many gigabytes, while a typical simulation generates about 25,000 such time-steps [40]. An earthquake simulation dataset is four-dimensional: it encodes three-dimensional information (the 3D coordinates of the sample points) at each time-step. Post-processing or visualization applications query the output, selecting the simulation results that correspond to ranges of the 4D coordinate space. As an example of such *range queries*, consider a “space-varying” query that retrieves the simulated values for all the ground points falling within a given 3D region for only a single time-step. Similarly, “time-varying” queries generate waveforms by querying the simulated values for a single point, but for a range of time-steps.

Unfortunately, naive data layout schemes lead to sub-optimal I/O performance. Optimizing for a given class of queries (e.g., the 3D spatial ranges), results in random accesses along the other dimensions (e.g., the time dimension). Due to the absence of an appropriate disk layout scheme, I/O performance is the bottleneck in earthquake simulation applications [40].

Organizing multidimensional data for efficient accesses is a core problem for several other scientific applications. High energy physics experiments will produce petabyte-scale datasets with hundreds of dimensions [33]. Astronomy databases like the Sloan Digital Sky Survey [15] record astronomical objects using several other attributes besides their coordinates (brightness in various wavelengths, redshifts, etc.). The data layout problem becomes more complex with an increasing number of dimensions because there are more query classes to be accommodated.

In addition to data-intensive science applications, large-scale multidimensional datasets are typically used

in On-Line Analytical Processing (OLAP) settings [14, 34, 39]. OLAP applications perform complex queries on large volumes of financial transactions data in order to identify sales trends and support decision-making. OLAP datasets have large numbers of dimensions, corresponding, for example, to product and customer characteristics, and to the time and geographic location of a sale. Performance of complex multidimensional analysis queries is critical for the success of OLAP and a large number of techniques have been proposed for organizing and indexing multidimensional OLAP data [7, 18, 32, 41].

## 2.2 Limitations of conventional placement

Efficient multidimensional data access relies on maintaining locality so that “neighboring” objects in the multidimensional (logical) space are stored in “neighboring” disk locations. Existing multidimensional layout techniques are based on the standard linear disk abstraction. Therefore, to take advantage of the efficient sequential disk access, neighboring objects in the multidimensional space must be stored in disk blocks with similar logical block numbers (*LBNs*). Space-filling curves, such as the Hilbert curve [17], Z-ordering [22] and Gray-coding [10] are mathematical constructs that map multidimensional points to a 1D (linear) space, so that nearby objects in the logical space are as close in the linear ordering as possible.

Data placement techniques that use space-filling curves rely on a simplified linear disk model, ignoring low-level details of disk performance. The resulting linear mapping schemes break sequential disk access, which can no longer be used for scans along any dimension, only to ensure that range queries do not result in completely random I/O. Furthermore, as analysis [20] and our experiments suggest, the ability of space-filling curves to keep neighbors in any dimensions physically close on the disk deteriorates rapidly as the number of dimensions increases. Our work revisits the simplistic disk model and removes the need for linear mappings. The resulting layout schemes maintain sequential disk bandwidth, while providing efficient access along any dimension, even for datasets with large dimensionality.

Besides space-filling curves, other approaches rely on parallel I/O to multiple disks. Declustering schemes [1, 4, 5, 11, 19, 23] partition the logical multidimensional space across multiple disks, so that range queries can take advantage of the aggregate bandwidth available.

## 2.3 Limitations of indexing

The need to efficiently support multidimensional queries has led to a large body of work on indexing. Multidimensional indexes like the R-tree [16] and its variants are disk-resident data structures that provide fast access

to the data objects satisfying a range query. With an appropriate index, query processing requires only a fraction of disk block accesses, compared to the alternative of exhaustively searching the entire dataset. The focus of multidimensional indexing research is on minimizing the number of disk pages required for answering a given class of queries [12].

Our work on disk layout for multidimensional datasets differs from indexing. It improves the performance of *retrieving* the data objects that match a given input query and not the efficiency of *identifying* those objects. For example, a range query on a dataset supported by an R-tree can result in a large number of data objects that must be retrieved. Without an appropriate data layout scheme, the data objects are likely to reside in separate pages at random disk locations. After using the index to identify the data objects, fetching them from the disk will have sub-optimal, random access performance. Multidimensional indexing techniques are independent of the underlying data layout and do not address the problem of maintaining access locality.

## 2.4 Storage-oriented approaches

Recently, researchers have focused on the lower level of the storage system in an attempt to improve performance of multidimensional queries [13, 27, 28, 38]. Part of the work revisits the simple disk abstraction and proposes to expand the storage interfaces so that the applications can be more intelligent. Schindler et al. [26] explored aligning accesses to disk drive track-boundaries to get rid of rotational latency. Gorbatenko et al. [13] and Schindler et al. [27] proposed a secondary dimension on disks, which they utilized to create a more flexible database page layout [30] for two-dimensional tables. Others have studied the opportunities of building two dimensional structures to support database applications with new alternative devices, such as MEMS-based storage devices [28, 38]. The work described in this paper challenges the underlying assumption of much of this previous work by showing that the characteristics of modern disk drives allow for efficient access to multiple dimensions, rather than just one or two.

## 3 Multidimensional disk access

The established view is that disk drives can efficiently access only one-dimensional data mapped to sequential logical blocks. This notion is further reinforced by the linear abstraction of disk drives as a sequence of fixed-size blocks. Behind this interface, disks use various techniques to further optimize for such sequential accesses. However, modern disk drives can allow for efficient access in more than one dimension. This fundamental change is based on two observations of technological trends in modern disks:

1. Short seeks of up to some cylinder distance,  $C$ , are dominated by the time the head needs to settle on a new track;
2. Firmware features internal to the disk can identify and thus access blocks that require no rotational latency after a seek.

By combining these two observations, it is possible to construct access patterns for efficient access to multidimensional data sets despite the current linear abstractions of storage systems.

This section describes the technical underpinnings of the mechanism that we exploit to preserve locality of multidimensional data on disks. We begin by describing some background of the mechanical operation of disks. We then analyze the technology trends of the relevant drive parameters, showing how the mechanism is enabled today and will continue to be enabled in future disks. Lastly, we combine the two to show how the mechanism itself works.

### 3.1 Disk background

**Positioning.** To service a request for data access, the disk must position the read/write head to the physical location where the data resides. First, it must move a set of arms to the desired cylinder, in a motion called seeking. Once the set of arms, each equipped with a distinct head for each surface, is positioned near the desired track, the head has to settle in the center of the track. After the head is settled, the disk has to wait for the desired sector to rotate underneath the stationary head before accessing it. Thus, the total positioning time is the sum of the seek time, settle time, and rotational latency components.

The dominant component of the total positioning time depends on the access pattern (i.e., the location of the previous request with respect to the next one). If these requests are to two neighboring sectors on the same track, no positioning overhead is incurred in servicing the second one. This is referred to as sequential access. When two requests are located on two adjoining tracks, the disk may incur settle time and some rotational latency. Finally, if the two requests are located at non-adjoining tracks, the disk may incur a seek, settle time, and possibly some rotational latency.

There are two possible definitions of adjoining tracks. They can be either two tracks with the same radius on different surfaces, or two neighboring tracks with different radii on the same surface. In the first case, different heads must be used to access the two tracks; in the second case, the same head is used for both. In both cases, the disk will have to settle the head above the correct track. In the former case, the settle time is incurred because (i) the two tracks on the two surfaces may not be perfectly aligned or round (called run out), (ii) the individual heads may not be perfectly stacked,

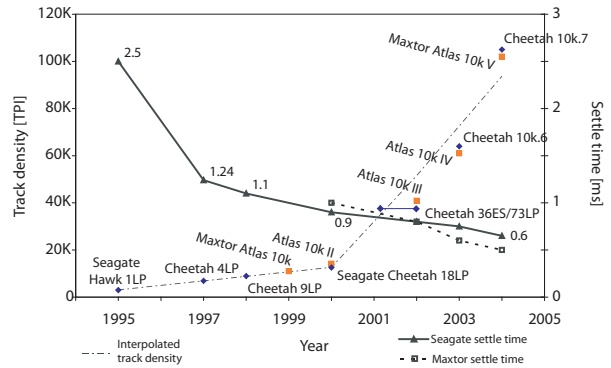


Figure 2: **Disk trends for 10,000 RPM disks.** Notice the dramatic increase in track density, measured in Tracks Per Inch (TPI), since 2000, while in the same period, head switch/settle time has improved only marginally.

and/or (iii) the arms may not be stationary (as any non-rigid body, they oscillate slightly). The former case is referred to as head switch between tracks of the same cylinder, while the latter is called a one cylinder seek.

**Request scheduling.** Disk drives use variants of shortest positioning time first (SPTF) request schedulers [29, 36], which determine the optimal order in which outstanding requests should be serviced by minimizing the sum of seek/settle time and rotational latency. To calculate the positioning cost, a scheduler must first determine the physical locations (i.e.,  $\langle$ cylinder, head, sector offset $\rangle$ ) of each request. It then uses seek time estimators encoded in the firmware routines to calculate the seek time and calculates residual rotational latency after a seek based on the offset of the two requests.

**Layout.** Disks map sequential *LBNs* to adjoining sectors on the same track. When these sectors are exhausted, the next *LBN* is mapped to a specific sector on the adjoining track to minimize the positioning cost (i.e., head switch or seek to the next cylinder). Hence, there is some rotational offset between the last *LBN* on one track and the next *LBN* on the next track. Depending on which adjoining track is chosen for the next *LBN*, this offset is referred to as track skew or cylinder skew.

### 3.2 Disk technology trends

The key to our method of enabling multidimensional access on disks is the relationship between two technology trends over the last decade: (1) the time for the disk head to settle at the end of a seek has remained largely constant, and (2) track density has increased dramatically. Figure 2 shows a graph of both trends for two families of (mostly) 10,000 RPM enterprise-class disks from two vendors, Seagate and Maxtor.

The growth of track density, measured in tracks per inch (TPI), has been one of the strongest trends in disk drive technology. Over the past decade, while settle time has decreased only by a factor of 5 [3], track densities

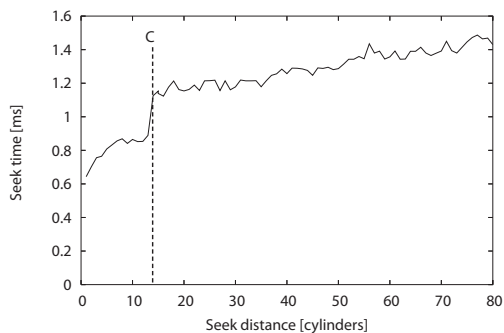


Figure 3: Atlas 10k III seek curve. First 80 cylinders.

experienced 35 fold increase, as shown in Figure 2. As track density continues to grow while settle time improves very little, more cylinders can be accessed in a given amount of time. With all else being equal, more data in the same physical area can be accessed in the same amount of time. However, increasing track density negatively impacts the settle time. With larger TPI, higher-precision controls are required, diminishing the improvements in settle time due to other factors. There are other factors that improve seek time such as using smaller platters [3], but these affect long and full-stroke seeks, whereas we focus on short-distance seeks.

In the past, the seek time for short distances between one and, say,  $L$  cylinders was approximately the square root of the seek distance [24]. However, the technology trends illustrated in Figure 2 lead to seek times that are nearly constant for distances of up to  $C$  cylinders, and which then increase as before for distances above  $C$  cylinders, as illustrated in Figure 1. Seeks of up to  $C$  cylinders are dominated by the time it takes a disk head to settle on the new track. These properties are confirmed by looking at the seek curve measured from a real disk, shown in Figure 3. The graph shows the seek curve for a Maxtor Atlas 10k III, a 10,000 RPM disk introduced in 2002. For this disk,  $C = 12$  and settle time is around 0.8 ms. For clarity, the graph shows seek time for distances up to 80 cylinders, even though it has over 31,000 cylinders in total (see Table 1).

While settle time has always been a factor in positioning disk heads, the dramatic increase in bit density over the last decade has brought it to the fore, as shown in Figure 2. At lower track densities (i.e., for disks introduced before 2000), only a single cylinder can be reached within a constant settle time. However, with the large increase in TPI since 2000, up to  $C$  can now be reached. Section 4.3 examines seek curves for more disks.

The increasing track density also influences how data is laid out on the disk. While in the past, head switches would be typically faster than cylinder switches, it is the other way around for today’s disks. With increasing TPI,

settling on the correct track with a different head/arm takes more time than simply settling on the adjoining track with the same head/arm assembly.

Disks used to lay out data first across all tracks of the same cylinder before moving to the next one, whereas most recent disks “stay” on the same surface for a number of cylinders, say  $C_{layout}$ , and move inward before switching to the next surface and going back. This mapping, which we term *surface serpentine*, also leverages the fact that seeks of up to  $C$  cylinders take a (nearly) constant amount of time. Put differently, the choice of  $C_{layout}$  must ensure that sequential accesses are still efficient even when two consecutive *LBNs* are mapped to tracks  $C_{layout}$  cylinders away. Figure 4 depicts the different approaches to mapping *LBNs* onto disk tracks.

### 3.3 Adjacent disk blocks

The combination of rapidly increasing track densities and slowly decreasing settle time leads to the seek curves shown above in which one of  $C$  neighboring cylinders can be accessed from a given starting point for equal cost. Each of these cylinders is composed of  $R$  tracks, and so, by extension, there are  $d = R \times C$  tracks that can be accessed from that starting point for equal cost. The values of  $C$  and  $d$  are related very simply, but we differentiate them to illuminate a subtle, but important, detail.

The value of  $C$  is a measure of *how far* the disk head can move (in cylinders) within the settle period, while the value of  $d$  is used to enumerate the number of adjacent blocks that can be accessed within those cylinders. While each of these  $d$  tracks contain many disk blocks, there is one block on each track that can be accessed immediately after the head settles on the destination track, with no additional rotational latency. We identify these blocks as being *adjacent* to the starting block.

Figure 5 shows a drawing of the layout of adjacent blocks on disk. For a given starting block, there are  $d$  adjacent disk blocks, one in each of the  $d$  adjacent tracks. For simplicity, we show a disk with only one surface, so, in this case,  $R$  is one, and  $d$  equals  $C$ . During the settle time, the disk rotates by a fixed number of degrees,  $W$ , determined by the ratio of the settle time to the rotational period of the disk. For example, with settle time of 1 ms and the rotational period of 6 ms (i.e., for a 10,000 RPM disk),  $W = 60^\circ$ . Therefore, all adjacent blocks have the same angular (physical) offset from the starting block.

As settle time is not entirely deterministic (i.e., due to external vibrations or thermal expansion), it is useful to add some extra conservatism to  $W$  to avoid rotational misses, which lead to long delays. Adding conservatism to the value of  $W$  increases the number of tracks,  $d$ , that can be accessed within the settle time at the cost of added rotational latency. In practice, disks also add some conservatism to the best-case settle time when determining

|                | <i>Model</i>  | <i>Year</i> | <i>TPI</i>     | <i>Cylinders</i> | <i>Surfaces</i> | <i>Max. Cap.</i> | <i>1-cyl Seek</i> | <i>Full Seek</i> |
|----------------|---------------|-------------|----------------|------------------|-----------------|------------------|-------------------|------------------|
| <b>Maxtor</b>  | Atlas 10k II  | 2000        | 14200          | 17337            | 20              | 73 GB            | 1 ms              | 12.0 ms          |
|                | Atlas 10k III | 2002        | 40000          | 31002            | 8               | 73 GB            | 0.8 ms            | 11.0 ms          |
|                | Atlas 10k IV  | 2003        | 61000          | 49070            | 8               | 147 GB           | 0.6 ms            | 12.0 ms          |
|                | Atlas 10k V   | 2004        | 102000         | 81782            | 8               | 300 GB           | 0.5 ms            | 12.0 ms          |
|                | Atlas 15k II  | 2004        | <i>unknown</i> | 48242            | 8               | 147 GB           | 0.5 ms            | 8.0 ms           |
| <b>Seagate</b> | Cheetah 4LP   | 1997        | 6932           | 6526             | 8               | 4.5 GB           | 1.24 ms           | 19.2 ms          |
|                | Cheetah 36ES  | 2001        | 38000          | 26302            | 4               | 36 GB            | 0.9 ms            | 11.0 ms          |
|                | Cheetah 73LP  | 2002        | 38000          | 29549            | 8               | 73 GB            | 0.8 ms            | 9.8 ms           |
|                | Cheetah 10k.6 | 2003        | 64000          | 49855            | 8               | 147 GB           | 0.75 ms           | 10.0 ms          |
|                | Cheetah 10k.7 | 2004        | 105000         | 90774            | 8               | 300 GB           | 0.65 ms           | 10.7 ms          |
|                | Cheetah 15k.4 | 2004        | 85000          | 50864            | 8               | 147 GB           | 0.45 ms           | 7.9 ms           |

Table 1: **Disk characteristics.** Data taken from manufacturers’ specification sheets. The listed seek times are for writes.

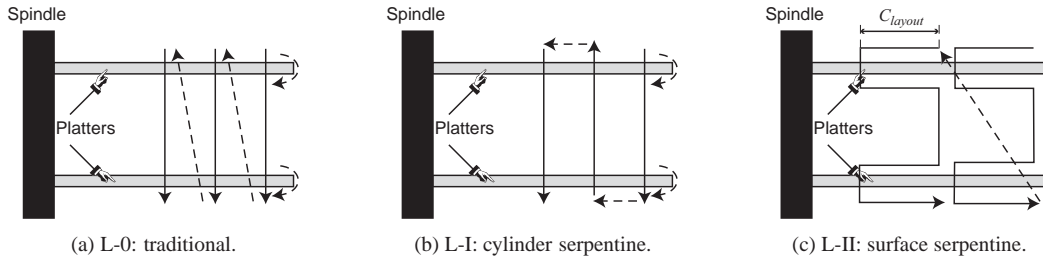


Figure 4: Layout mappings adopted by various disk drives.

cylinder and track skews for mapping *LBNs* to physical locations. For our example Atlas 10k III disk, the cylinder and track skews are  $61^\circ$  and  $68^\circ$ , respectively, or 1.031 ms and 1.141 ms, even though the measured settle time is less than 0.8 ms. This extra buffer of about  $14^\circ$  ensures that the disk will not miss a rotation during sequential access when going from one track to the next.

Note that depending on the mapping of logical blocks (*LBNs*) to physical locations these blocks can appear to an application either sequential or non-contiguous. The choice is simply based on how a particular disk drive does its low-level logical-to-physical mapping. For example, a pair of sequential *LBNs* mapped to two different tracks or cylinders are still adjacent, according to our definition, as are two specific non-contiguous *LBNs* mapped to two nearby tracks.

Accessing successive adjacent disk blocks enables *semi-sequential* disk access [13, 27], which is the second-most efficient disk access method after pure sequential access. The delay between each access is equal to a disk head settle time, which is the minimum mechanical positioning delay the disk can offer. However, the semi-sequential access introduced previously utilizes only one of the adjacent blocks for efficiently accessing 2D data structures. This work shows how to use up to  $d$  adjacent blocks to improve access efficiency for multidimensional datasets.

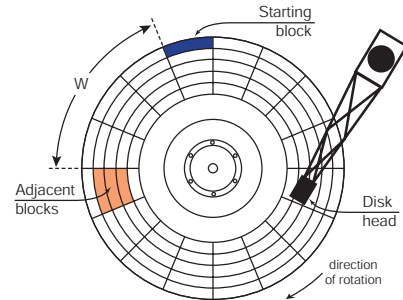


Figure 5: Location of adjacent blocks.  $W = 67.5^\circ$  and  $C = 3$ .

## 4 Determining $d$

The previous section defined the adjacency relationship and identified the disk characteristics which enable access to adjacent blocks. We now describe two methods for determining the value of  $d$ . The first method we use analyzes the extracted seek curves and drive parameters to arrive at an estimate for  $C$  (and, by extension,  $d$ ), and the second method empirically measures  $d$  directly. We evaluate and cross-validate both methods for a set of disk drives from two different vendors.

### 4.1 Experimental setup

All experiments described here are conducted on a two-way 1.7 GHz Pentium 4 Xeon workstation running Linux kernel 2.4.24. The machine has 1024 MB of

main memory and is equipped with one Adaptec Ultra160 Wide SCSI adapter connecting the disks. For our experiments, some of our disks have fewer platters than the maximum supported, which are listed in Table 1. Most enterprise drives are sold in families supporting a range of capacities, in which the only difference is the number of platters in the drive. Specifically, our Cheetah 36ES and Atlas 10k III have two platters, while the Atlas 10k IV, Atlas 10k V, Cheetah 10k.7, and Cheetah 15k.4 disks have only one platter. All but one disk have the same total capacity of 36.7 GB; the Cheetah 10k.7 is a 73 GB disk. Requests are issued to the disks via the Linux SCSI Generic driver and are timed using the CPU’s cycle counter. All disks had their default cache mode page settings with both read and write cache enabled.

## 4.2 Seek measurements

To determine the proper values of  $C$  and  $d$  based on the disk’s characteristics, we need to measure its seek profile. Since we do not have access to the disk firmware, we have to determine it empirically. We first obtain mappings of each  $LBN$  to its physical location, given by the  $\langle \text{cylinder, head, sector} \rangle$  tuple. We use the SCSI address translation mode page (0x40h) and `MODE SELECT` command. With a complete layout map, we can choose a pair of tracks for the desired seek distance and measure how long it takes to seek from one to the other.

To measure seek time, we choose a pair of cylinders separated by the desired distance, issue a pair of read commands to sectors in those cylinders and measure the time between their completions. We choose a fixed  $LBN$  on the source track and successively change the value of the  $LBN$  on the second track, each time issuing a pair of requests, until we find at the lowest time between request completions. This technique is called the Minimal Time Between Request Completions (MTBRC) [37]. The seek time we report is the average of 6 trials of MTBRC, each with randomly-chosen starting locations spread across the entire disk. Note that the MTBRC measurement subtracts the time to read the second sector as well as bus and system overheads [37].

## 4.3 Seek profile analysis

The first method we use to determine  $C$  (and thus  $d$ ) is based on analyzing the seek profile of a disk. Figure 6 shows seek profiles of the disk drives we evaluated for small cylinder distances. Note that extracted profiles have very similar shape, especially among drives from the same vendor. The one-cylinder seek time is the lowest, as expected. For distances of two and more cylinders, the seek time rises rapidly for a few cylinders, but then levels off for several cylinders before it experiences a large increase between distance of  $i$  and  $i + 1$  cylin-

ders. After this inflection point, which is  $C$ , seek time rises gradually with increasing seek distance.

Note that the seek profile of some disks have more than one “plateau” and, thus, several possible values of  $C$ . When determining our value of  $C$  we chose the discontinuity point where seek times after the distance of  $C$  are at least 80% more than the one-cylinder seek time, while seek times of up to  $C$  are at most 60% larger than the one-cylinder seek time. Note that this is just one way of choosing the appropriate value of  $C$ . In practice, disk designers are likely to choose a value manually based on the physical disk parameters, just as they choose the value of track and cylinder skew. In either case, the choice of  $C$  is a trade-off between larger value of  $d$  (which increases the number of potential dimensions that can be accessed efficiently), and the efficiency of accesses to individual adjacent blocks.

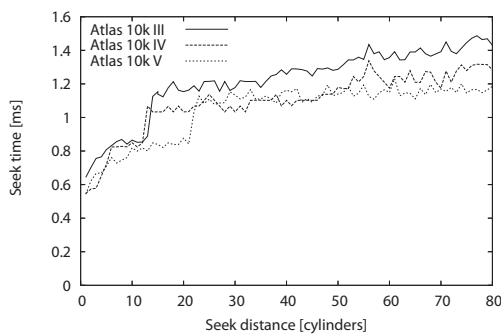
Using their measured seek curves, we now determine suitable values of  $C$  for six recent disk drives. Recall that  $C$  is the maximal seek distance in cylinders for which positioning time is (nearly) constant. Table 2 lists the value for each disk drive determined as the inflection point/discontinuity in the seek profile. The other pair of numbers in the table shows the percentage difference between seek time for distance of 1 cylinder and the distance of respectively  $C$  and  $C+1$  cylinders, highlighting this discontinuity.

First, as expected, for more recent disk drives the value of  $C$  increases. Second, the difference between one-cylinder and  $C$ -cylinder seek times is about 50%. And finally, the difference in seek time between a one- and  $C+1$ -cylinder seek is significant: between  $1.7\times$  and  $2\times$  the value of the one-cylinder seek.

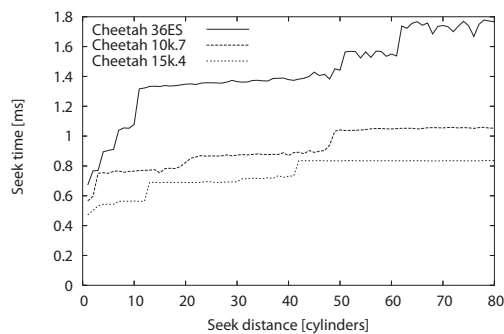
Once we have determined a value for  $C$ , we simply multiply by the number of surfaces in the disk to arrive at  $d$ . Figure 7 depicts the values of  $d$  for our disks. For each of the disks, we use the value of  $C$  from Table 2 and multiply it by the maximal number of surfaces each disk can have. From Table 1, for all but the Cheetah 36ES,  $R = 8$ . We plot the value of  $d$  as a function of year when the particular disk model was introduced. For years with multiple disks, we average the value of  $d$  across all analyzed disk models. Confirming our trend analysis, the value of  $d$  increases from 40 in year 2001 to almost 300 in year 2004. Recall that the value of  $d$  is proportional to the number of surfaces in the disk,  $R$ , and that the lower-capacity versions of the disk drives (such as those in our experiments) will have smaller values of  $d$  than those with more platters.

## 4.4 Measuring $C$ directly

We now verify our previous method of determining  $C$  by measuring it directly. We measure the value for  $d$  rather than  $C$ , but, of course,  $C$  can easily be determined



(a) Recent Maxtor enterprise-class disks



(b) Recent Seagate enterprise-class disks

Figure 6: Measured seek profiles. Only the first 80 cylinders are shown.

| Disk Model    | Year | C  | 1-cyl seek diff. vs. |           |
|---------------|------|----|----------------------|-----------|
|               |      |    | C-cyl                | (C+1)-cyl |
| Atlas 10k III | 2002 | 13 | 38%                  | 76%       |
| Atlas 10k IV  | 2003 | 12 | 52%                  | 98%       |
| Atlas 10k V   | 2004 | 21 | 55%                  | 91%       |
| Cheetah 36 ES | 2001 | 10 | 59%                  | 94%       |
| Cheetah 10k.7 | 2004 | 49 | 44%                  | 80%       |
| Cheetah 15k.4 | 2004 | 42 | 55%                  | 78%       |

Table 2: Estimated values of  $C$  based on seek profiles. The seek times compare the extracted value of 1-cylinder seek and  $C$ -cylinder seek. The last column lists the percentage increase between 1-cylinder and  $C$ -cylinder seek time.

by dividing  $d$  by the number of surfaces in the disk,  $R$ . We use the low-level layout model and the value of  $W$  to identify those blocks that are adjacent to the starting block. The experiment chooses a random starting block and a destination block which is  $i$  tracks away and is skewed by  $W$  degrees relative to the starting block.

We issue the two requests to the disk simultaneously and measure the response time of each one individually. If the difference in response time is equal to the settle time of the disk, then the two blocks are truly adjacent, and  $i < d$ . We increase  $i$  until the response time of the second request increases significantly, beyond the rotational period of the disk. This value of  $i$  is the maximum distance that the disk head can move and still access adjacent blocks without missing rotations, so  $d = i - 1$ .

Adding conservatism to the rotational offset,  $W$ , provides a useful buffer because of nondeterminism in the seek time. We found this to be especially true when experimenting with real disks, so our baseline values for  $W$  include an aggressive value of  $10^\circ$  for conservatism. Recall that the Atlas 10k III layout, for example, uses a buffer of  $14^\circ$  for track and cylinder skews.

Larger conservatism can increase the value of  $d$  at the expense of additional rotational latency and, hence, lower semi-sequential efficiency. Conceptually, this is

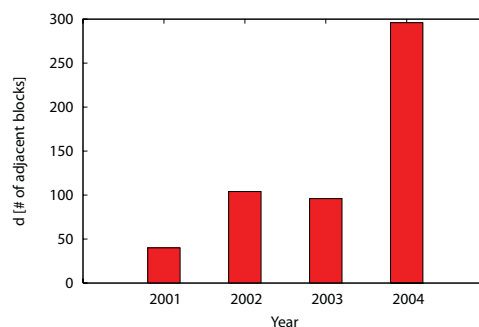


Figure 7: The trend in estimated value of  $d$ . The reported values are based on our estimated values of  $C$  multiplied by the disk’s maximal number of surfaces. For years where we measured data from more than one disk model, we report the average value of  $d$ .

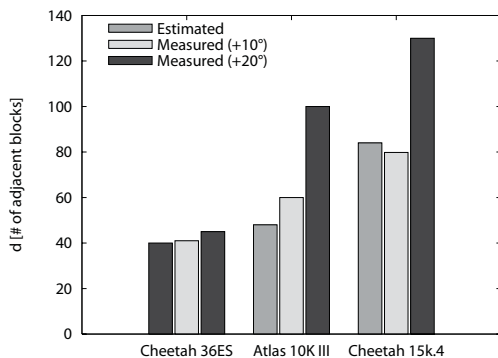
analogous to moving to the right along the seek profile past the discontinuity point. Larger values of  $d$ , in turn, allow mappings of data sets with many more dimensions, while maintaining the same efficiency for accesses to all  $N - 1$  dimensions. Even though, more conservatism (and larger  $d$ ) lowers the achieved semi-sequential bandwidth, it considerably increases the value of  $d$  as illustrated in Figure 8.

Figure 8(a) shows the comparison between the value of  $d$  based on our seek profile estimates of  $C$  reported in Table 2 and our measured values using the above approach. For each disk, we show three bars. The first bar, labeled “Estimated”, is the value of the estimated  $d$ . The second and third bar, labeled “Measured ( $+10^\circ$ )” and “Measured ( $+20^\circ$ )”, show the measured value with a conservatism of  $10^\circ$  and  $20^\circ$ , respectively, added to  $W$ . The “Estimated” values are based on our measurements from our disks, which have fewer platters than the models reported in Table 1. In contrast, the values reported in Figure 7 are based on disks with maximal capacities.

#### 4.5 Eliminating rotational latency

A key feature of adjacent blocks is that, by definition, they can be accessed immediately after the disk head





(a) Comparison of estimated and measured  $d$ .

| Disk Model    | $W$ | Extra | $d$ | Access time |
|---------------|-----|-------|-----|-------------|
| Atlas 10k III | 68° | 0°    | 25  | 0.95 ms     |
|               |     | 10°   | 60  | 1.00 ms     |
|               |     | 20°   | 100 | 1.25 ms     |
| Cheetah 36ES  | 59° | 0°    | 20  | 0.85 ms     |
|               |     | 10°   | 35  | 1.00 ms     |
|               |     | 20°   | 45  | 1.20 ms     |
| Cheetah 15k.4 | 70° | 0°    | 18  | 0.85 ms     |
|               |     | 10°   | 80  | 0.85 ms     |
|               |     | 20°   | 130 | 0.85 ms     |

(b) Increasing conservatism increases  $d$  and access time.

Figure 8: Comparison of estimated and measured  $d$ .

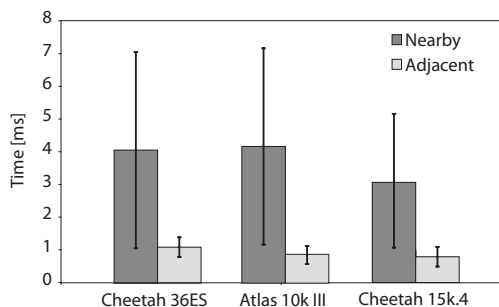


Figure 9: **Quantifying access times.** This graph compares the access times to blocks located within  $C$  cylinders. For the first two disks, the average rotational latency is 3 ms, for Cheetah 15k.4, it is 2 ms.

settles, without any rotational latency. To quantify the benefits of eliminating rotational latency, we compare adjacent access to simple nearby access within  $d$  tracks. Without explicit knowledge of adjacency, accessing each pair of nearby blocks will incur, on average, rotational latency of half a revolution, in addition to the seek time equivalent to the settle time. If these blocks are specifically chosen to be adjacent, then the rotational latency is eliminated and the access is much more efficient.

As shown in Figure 9, adjacent access outperforms nearby access by a factor of 4 thanks to the elimination of all rotational latency. Additionally, the access time for the nearby case varies considerably due to variable rotational latency, while the access time variability is much smaller for the Adjacent case; it is entirely due to the difference in seek time within the  $C$  cylinders, as depicted by the error bars.

## 5 Expressing adjacency to applications

The previous sections detailed the principles behind efficient access to  $d$  adjacent blocks and demonstrated that existing functions inside disk firmware (e.g., request schedulers) can readily identify and access these blocks. However, today’s interfaces do not expose these blocks outside the disk. This section presents the method we

use for exposing adjacent blocks so that applications can use them for efficient access to multidimensional data. It first describes how individual disks can cleanly expose adjacent blocks, and then shows how to combine such information from individual disks comprising a logical volume and expose it using the same abstractions.

### 5.1 Exposing adjacent blocks

To allow for efficient access, the linear abstraction of disk drives sets an explicit contract between contiguous  $LBNs$ . To extend efficient access to adjacent blocks, we need to expose explicit relationships among the set of adjacent  $LBNs$  that are *non-contiguous*.

To expose the adjacency relationships, we need to augment the existing interface with one function, here called GETADJACENT. Given an  $LBN$ , this function returns a list of adjacent  $LBNs$  and can be implemented similarly to a  $LBN$ -to-physical address translation, i.e., a vendor-specific SCSI mode page accessed with the MODE SELECT command. The application need not know the reasons how or why the returned  $d$  disk blocks are adjacent, it just needs to have them identified through the GETADJACENT function.

A useful (conceptual) way to express the adjacency relationships between disk blocks is by constructing adjacency graphs, such as that shown in Figure 10. The graph nodes represent disk blocks and the edges connect blocks that are adjacent. The graph in the figure shows two levels of adjacency: the root node is the starting block, the nodes in the intermediate level are adjacent to that block, and the nodes in the bottom level are adjacent to the blocks in the intermediate level. Note that adjacent sets of adjacent blocks (i.e., those at the bottom level of the graph) overlap. For brevity, the graph shows only the first 6 adjacent blocks (i.e.,  $d = 6$ ), even though  $d$  is considerably larger for this disk, as described in Section 4. With the concept of adjacent blocks, applications can lay out and access multidimensional data with the existing 1D abstraction of the disk. This is pos-

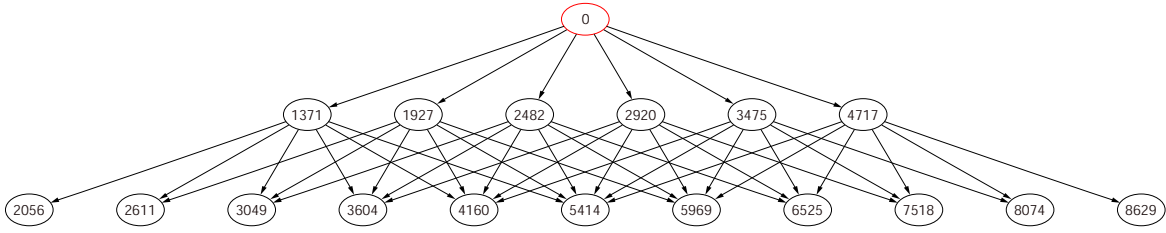


Figure 10: Adjacency graph for LBN 0 of Atlas 10k III. Only two levels adjacent blocks are shown. The LBNs are shown inside nodes.

sible through explicit mapping of particular points in the data’s multidimensional space to particular LBNs identified by the disk drive.

## 5.2 Identifying adjacent blocks

Since current disk drives do not expose adjacent blocks and we do not have access to disk firmware to make the necessary modifications, we now describe an algorithm for identifying them in the absence of the proper storage interface functions. The algorithm uses a detailed model of low-level disk layout borrowed from a storage system simulator called DiskSim [8]. The parameters can be extracted from SCSI disks by previously published methods [25, 35, 37]. The algorithm uses two functions that abstract the disk-specific details of the disk model: GETSKEW(*lbn*), which returns the physical angle between the physical location of an LBN on the disk and a “zero” position, and GETTRACKBOUNDARIES(*lbn*), which returns the first and the last LBN at the ends of the track containing *lbn*.

For convenience, the algorithm also defines two parameters. First, the parameter *T* is the number of disk blocks per track and can be found by calling GETTRACKBOUNDARIES, and subtracting the low LBN from the high LBN. Of course, the value of *T* varies across zones of an individual disk, and will have to be determined for each call to GETADJACENT. Second, the parameter *W* defines the angle between a starting block and its adjacent blocks. This angle can be found by calling the GETSKEW function twice for two consecutive LBNs mapped to two different tracks and computing the difference; disks skew the mapping of LBNs on consecutive tracks by *W* degrees to account for settle time and to optimize sequential access.

The GETADJACENT algorithm, shown in Figure 11, takes as input a starting LBN (*lbn*) and finds the adjacent LBN that is *W* degrees ahead and *step* tracks away. Every disk block has an adjacent block within the *d* closest tracks, so the entire set of adjacent blocks is found by calling GETADJACENT for increasing values of *step* from 1 to *d*.

```

/* Find an LBN adjacent to lbn and step tracks away */
L := GETADJACENT(lbn, step) :
  /* Find the required skew of target LBN */
  target_skew := (GETSKEW(lbn) + W) mod 360

  /* Find the first LBN in target track */
  base_lbn := lbn + (step * T)
  {low, high} := GETTRACKBOUNDARIES(base_lbn)

  /* Find the minimum skew of target track */
  low_skew := GETSKEW(low)

  /* Find the offset of target LBN from the start of target track */
  if (target_skew > low_skew) then
    offset_skew := target_skew - low_skew
  else
    offset_skew := target_skew - low_skew + 360
  end if

  /* Convert the offset skew into LBNs */
  offset_lbn := (offset_skew/360) * T
  RETURN(low + offset_lbn)

/* Find the physical skew of lbn, measured in degrees */
A := GETSKEW(lbn)

/* Find the boundaries of the track containing lbn */
{L, H} := GETTRACKBOUNDARIES(lbn)

T: Track length - varies across zones of the disk
W: Skew to add between adjacent blocks, measured in degrees

```

Figure 11: Algorithm for the GETADJACENT function.

## 5.3 Logical volumes

So far, we have discussed how to expose adjacent blocks to applications from a single disk drive. However, large storage systems combine multiple disks into logical volumes. From our perspective, a logical volume manager (LVM) adds nothing more than a level of indirection through mapping of a volume LBN (VLBN) to the LBNs of individual disks (DLBN). Given a set of adjacent blocks, an LVM can choose an explicit grouping of LBNs across all underlying *k* disks. The *d* VLBNs exposed via GETADJACENT are the adjacent blocks of a particular disk’s DLBN mapped to a given VLBN by the LVM. To an application, a multi-disk logical volume will appear as a (bigger and faster) disk, whose adjacent blocks set has cardinality *d*.

Since existing disks do not implement the `GETADJACENT` and `GETTRACKBOUNDARIES` functions, in our prototype implementation, a shim layer below our LVM extracts the information from the disk drives. It does so when the logical volume is initially created and provides these functions for the given disk. The LVM then stripes contiguous *VLBNs* across  $k$  individual disks and exposes to applications a set of  $d$  adjacent blocks in the *VLBN* space through the `GETADJACENT` function.

Much like other disk array logical volumes [6, 27], our LVM matches stripe units to track sizes for efficient sequential access. Our LVM exposes to applications the stripe unit size,  $T$ , through the `GETTRACKBOUNDARIES` function. It can adopt common RAID 1 and RAID 5 protection schemes and utilize multi-zone disks with defective blocks in a fashion similar to previous work [27].

For multi-zone disks, our LVM can either create multiple logical volumes, one for each zone, or create one logical volume that spans multiple zones. In the latter case, our LVM uses varies the value of  $T$  according to the number of sectors per track in the disk’s zone to which the *VLBNs* is mapped. Put differently, in this approach, which we adopt for our experiments, a single logical volume has variable “stripe unit” size and our mappings of multidimensional data use the information exposed through the `GETTRACKBOUNDARIES` function to determine the proper mapping along the one dimension (see Section 6 for more details). Finally,  $d$  does not depend on the number of zones; it is strictly a function of track density (TPI) and the seek profile, which is fixed for a given disk and does not change with the location of the track.

## 6 Multidimensional data placement

This section demonstrates on 3D and 4D datasets how applications can utilize the adjacent blocks and the parameter  $T$  datasets onto disks in a way that preserves spatial locality. Through experiments with real disks and various workloads we show that this new mapping scheme outperforms existing schemes.

### 6.1 Data placement that preserves locality

To demonstrate the efficiency of accesses to adjacent blocks, we compare two existing mapping schemes for multidimensional data, *Naive* and *Hilbert*, with a new mapping scheme, called *MultiMap*. The *Naive* scheme linearizes the dataset along a chosen primary dimension (e.g.,  $X$  or time). The *Hilbert* scheme orders the points according to their Hilbert curve values.

The *MultiMap* mapping scheme uses adjacent blocks to preserve spatial locality of multidimensional data on the disk(s). It first partitions the multidimensional data space into smaller chunks, called *basic cubes*, and then

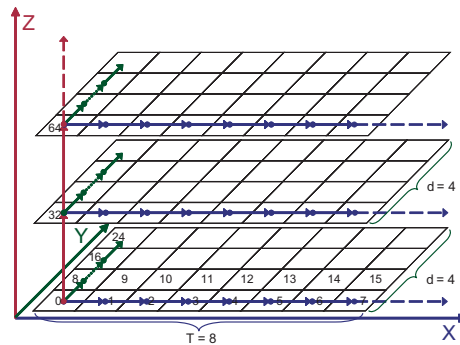


Figure 12: **Example of mapping a 3D dataset using *MultiMap*.** Each row in the graph represents a disk track with a length of 8 and each cell corresponds to a disk block whose *lbn* is the number inside the box. Suppose the value of  $d$  is 4. Dimension  $X$  is mapped to the sequential blocks on the same track. Dimension  $Y$  is mapped to the sequence of the first adjacent blocks. For example, *lbn* 8 is the first adjacent block of *lbn* 0 and *lbn* 16 is the first adjacent block of *lbn* 8, etc. Dimension  $Z$  is mapped to the sequence of the 4th adjacent blocks. For instance, *lbn* 32 is the 4th adjacent block of *lbn* 0 and *lbn* 64 is the 4th adjacent of *lbn* 32. In this way, *MultiMap* utilizes the adjacent blocks with different steps to preserve locality on the disk.

maps all the points within a basic cube into disk blocks on a single disk. Taking a 3D dataset as an example, *MultiMap* first maps points in the  $X$  dimension to  $T$  sequential *LBNs* so that accesses along  $X$  can take advantage of the full sequential bandwidth of the disk. Points along the  $Y$  dimension are mapped to the sequence of the first adjacent blocks. Lastly, the  $Z$  dimension is mapped to the sequence of  $d$ -th adjacent blocks, as Figure 12 shows. The sequence of adjacent blocks can be easily obtained by calling `GETADJACENT` repeatedly. With an LVM comprised of several disks, two “neighboring” basic cubes are mapped to two different disks and the basic cube becomes a multidimensional stripe unit.

*MultiMap* preserves the spatial locality in the sense that neighboring points in the geometric space will be stored in disk blocks that are adjacent to each other, allowing for access with minimal positioning cost. Since accessing the first adjacent block and the  $d$ -th adjacent block has the same cost, we can access up to  $d$  separate points that are equidistant from a starting point. This mapping preserves the spatial relationship that the next point along  $Y$  and the next point along  $Z$  are equidistant (in terms of positioning cost) to the same starting point. Retrieval along the  $X$  dimension result in efficient sequential access; retrieval along  $Y$  or  $Z$  result in semi-sequential accesses which are much more efficient than random or even nearby access, as shown in Figure 9.

Note that *MultiMap* is not a simple mapping of the 3D data set to the  $\langle \text{cylinder}, \text{head}, \text{sector} \rangle$  tuple representing the coordinates of the physical blocks on disk. *MultiMap* provides a general approach for mapping  $N$ -dimensional data sets to adjacent blocks. For a given disk, the maximum number of dimensions that can be

mapped efficiently is limited by  $d$  for that disk, such that  $N \leq \log_2(d) + 2$ . As the focus of this work is the analysis of the principles behind multidimensional access and not the general data layout algorithm, we provide the generalized algorithm, its derivation, and the analysis of its limits elsewhere [31].

## 6.2 Experimental setup

Our experimental setup uses the same hardware configuration as in Section 4. Our prototype system consists of two software components running on the same host machine: a logical volume manager (LVM) and a database storage manager. In a production system, the LVM would likely reside inside a storage array system separate from the host machine. The prototype LVM implements the GETADJACENT algorithm and exports a single logical volume mapped across multiple disks. The database storage manager maps multidimensional datasets by utilizing the GETADJACENT and GETTRACKBOUNDARIES functions provided by the LVM. Based on the query type, it issues appropriate I/Os to the LVM, which then breaks these I/Os into proper requests to individual disks. Even when such requests are issued out of order, the disk firmware scheduler will reorder them to minimize the total positioning cost.

The datasets used for our experiments are stored on multiple disks in our LVM. Akin to commercial disk arrays, the LVM uses disks of the same type and utilizes only a part (slice) of the disk’s total space [9]. The slices in our experiments are slightly less than half of the total disk capacity and span one or more zones.

Even though our LVM generates requests to all the disks during our experiments, we report performance results for only a single disk. The reason is that we examine average I/O response times, which depend only on the characteristics of a single disk drive. Using multiple drives improves the overall throughput, but does not affect the relative performance comparisons of the three mappings that our database storage manager implements: *Naive*, *Hilbert*, and *MultiMap*.

We evaluate two types of spatial queries. *Beam queries* are one-dimensional queries retrieving data points along lines parallel to the cardinal dimensions of the dataset. Range queries, called *p%-length cube queries*, fetch a cube with an edge length equal to the  $p\%$  of the dataset’s edge length.

## 6.3 Results using a 3D dataset

The 3D dataset used in this experiment contains  $1024 \times 1024 \times 1024$  cells, where each cell maps to a distinct *LBN* of the logical volume and contains as many data points as can fit. We partition the space into chunks that each fit on a portion of a single disk. For both disks, *MultiMap* uses  $d = 128$  and conservatism of  $30^\circ$ .

**Beam queries.** The results for beam queries are presented in Figure 13(a). We run beam queries along all three dimensions,  $X$ ,  $Y$ , and  $Z$ , and the graphs show the average I/O time per cell (disk block). As expected, the *MultiMap* model delivers the best performance for all dimensions. It matches the streaming performance of *Naive* along  $X$ . More importantly, *MultiMap* outperforms *Hilbert* for  $Y$  and  $Z$  by 25%—35% and *Naive* by 62%–214% for the two disks. Finally, *MultiMap* achieves almost identical performance on both disks unlike *Hilbert* and *Naive*. That is because these disks have comparable settle times, which affect the performance of accessing adjacent blocks for  $Y$  and  $Z$ .

**Range queries.** The first set of three bars, labeled 1% in Figure 13(b), shows the performance of 1%-length cube queries expressed as their total runtime. As before, the performance of each scheme follows the trends observed for the beam queries. *MultiMap* improves the query performance (averaged across the two disks and the three query types) by 37% and 11% respectively compared to *Naive* and *Hilbert*. Both *MultiMap* and *Hilbert* outperform *Naive* as it cannot employ sequential access for range queries. *MultiMap* outperforms *Hilbert*, as *Hilbert* must fetch some cells from physically distant disk blocks, although they are close in the original dataset. These jumps make *Hilbert* less efficient compared to *MultiMap*’s semi-sequential accesses.

To examine the sensitivity of the cube query size, we also run 2%-length and 3%-length cube queries, whose results are presented in the second and third sets of bars in Figure 13(b). The trends are similar, with *MultiMap* outperforming *Hilbert* and *Naive*. The total run time increases because each query fetches more data.

## 6.4 Results using a 4D dataset

In earthquake simulation, we use a 3D grid to model the 3D region of the earth. The simulation computes the motion of the ground at each node in the grid, for a number of discrete time steps. The 4D simulation output contains a set of 3D grids, one for each step.

Our dataset is a  $2000 \times 64 \times 64 \times 64$  grid modeling a 14 km deep slice of earth of a  $38 \times 38$  km area in the vicinity of Los Angeles with a total size of 250 GB of data. 2000 is the total number of time steps. We choose time as the primary dimension for the *Naive* and the *MultiMap* schemes and partition the space into chunks that fit in a single disk.

The results, presented in Figure 14, exhibit the same trends as the 3D experiments. The *MultiMap* model again achieves the best performance for all beam and range queries. In Figure 14(a), the unusually good performance of *Naive* on  $Y$  is due to a particularly fortunate mapping that results in strided accesses that do not incur any rotational latency. The ratio of strides to track

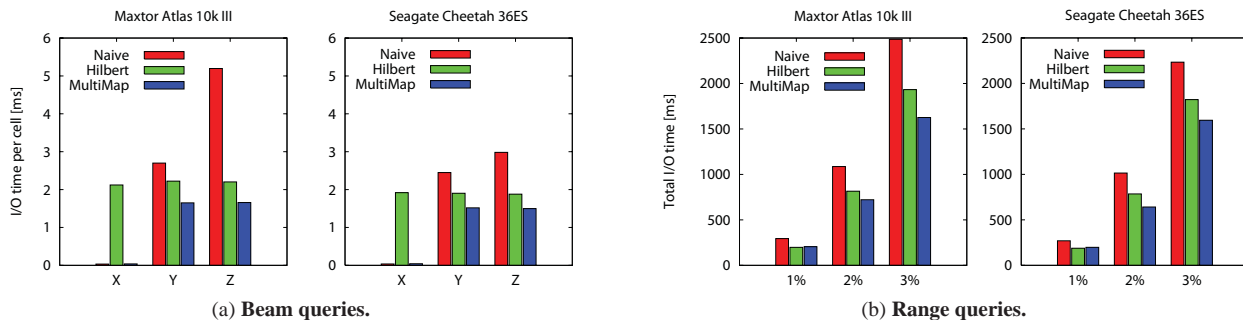


Figure 13: Performance using the 3D spatial dataset.

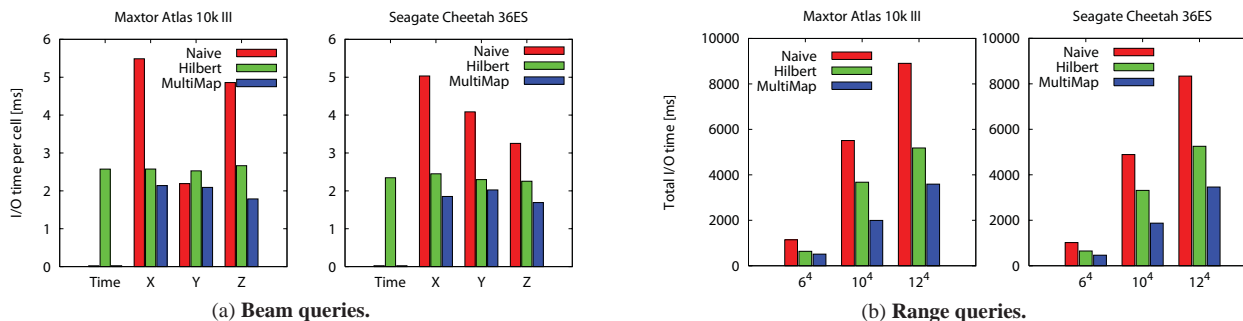


Figure 14: Performance using the 4D earthquake dataset.

sizes also explains the counterintuitive trend of the *Naive* scheme’s performance on the Cheetah disk where *Z* outperforms *Y*, and *Y* outperforms *X*. The range queries, shown in Figure 14(b), perform on both disks as expected from the 3D case. In summary, *MultiMap* is efficient for processing queries against spatio-temporal datasets, such as this earthquake simulation output, and is the only scheme that can combine streaming performance for time-varying accesses with efficient spatial access, thanks to the preservation of locality on disk.

## 7 Conclusion

The work presented here exploits disk drive technology trends. It improves access to multidimensional datasets by allowing the spatial locality of the data to be preserved in the disk itself. Through analysis of the characteristics of several state-of-the-art disk drives, we show how to efficiently access non-contiguous adjacent *LBNs*, which are hundreds of tracks away. Such accesses can be readily realized with the existing disk firmware functions and mappings of *LBNs* to physical locations.

Using our prototype implementation built with real, off-the-shelf disk drives, we demonstrate that applications can utilize streaming bandwidth for accesses along one dimension and efficient semi-sequential accesses in the other  $N - 1$  dimensions. To the best of our knowledge, this is the first approach that can preserve spatial locality of stored multidimensional data, thus improving performance over current data placement techniques.

## Acknowledgments

We thank John Bucy for his years of effort developing and maintaining the disk models that we use for this work. We thank the members and companies of the PDL Consortium (including APC, EMC, EqualLogic, Hewlett-Packard, Hitachi, IBM, Intel, Microsoft, Network Appliance, Oracle, Panasas, Seagate, and Sun) for their interest, insights, feedback, and support. We also thank IBM, Intel, and Seagate for hardware donations that enabled this work. This work is funded in part by NSF grants IIS-0133686 and CCR-0205544, by a Microsoft Research Grant, and by an IBM faculty partnership award.

## References

- [1] K. A. S. Abdel-Ghaffar and A. E. Abbadi. Optimal Allocation of Two-Dimensional Data. *International Conference on Database Theory* (Delphi, Greece), pages 409-418, January 8-10, 1997.
- [2] V. Akcelik, J. Bielak, G. Biros, I. Epanomeritakis, A. Fernandez, O. Ghattas, E. J. Kim, J. Lopez, D. O’Hallaron, T. Tu, and J. Urbanic. High Resolution Forward And Inverse Earthquake Modeling on Terascale Computers. *ACM/IEEE Conference on Supercomputing*, page 52, 2003.
- [3] D. Anderson, J. Dykes, and E. Riedel. More than an interface: SCSI vs. ATA. *Conference on File and Storage Technologies* (San Francisco, CA, 31 March–02 April 2003), pages 245–257. USENIX Association, 2003.
- [4] M. J. Atallah and S. Prabhakar. (Almost) Optimal Parallel Block Access for Range Queries. *ACM SIGMOD-SIGACT-SIGART Symposium on Principles of Database Systems* (Dallas, Texas, USA), pages 205-215. ACM, 2000.

- [5] R. Bhatia, R. K. Sinha, and C.-M. Chen. Declustering Using Golden Ratio Sequences. *ICDE*, pages 271–280, 2000.
- [6] P. M. Chen and D. A. Patterson. *Maximizing performance in a striped disk array*. UCB/CSD 90/559. Computer Science Div., Department of Electrical Engineering and Computer Science, University of California at Berkeley, February 1990.
- [7] P. M. Deshpande, K. Ramasamy, A. Shukla, and J. F. Naughton. Caching multidimensional queries using chunks. *ACM SIGMOD International Conference on Management of Data*, pages 259–270. ACM Press, 1998.
- [8] The DiskSim Simulation Environment (Version 3.0). <http://www.pdl.cmu.edu/DiskSim/index.html>.
- [9] EMC Corporation. *EMC Symmetrix DX3000 Product Guide*, [http://www.emc.com/products/systems/DMX\\_series.jsp](http://www.emc.com/products/systems/DMX_series.jsp), 2003.
- [10] C. Faloutsos. Multiattribute hashing using Gray codes. *ACM SIGMOD*, pages 227–238, 1986.
- [11] C. Faloutsos and P. Bhagwat. Declustering Using Fractals. *International Conference on Parallel and Distributed Information Systems* (San Diego, CA, USA), 1993.
- [12] V. Gaede and O. Günther. Multidimensional Access Methods. *ACM Comput. Surv.*, **30**(2):170–231, 1998.
- [13] G. G. Gorbatenko and D. J. Lilja. *Performance of two-dimensional data models for I/O limited non-numeric applications*. Laboratory for Advanced Research in Computing Technology and Compilers Technical report ARCTiC-02-04. University of Minnesota, February 2002.
- [14] J. Gray, A. Bosworth, A. Layman, and H. Pirahesh. Data Cube: A Relational Aggregation Operator Generalizing Group-By, Cross-Tab, and Sub-Total. *ICDE*, pages 152–159. IEEE Computer Society, 1996.
- [15] J. Gray, D. Slutz, A. Szalay, A. Thakar, J. vandenBerg, P. Kunszt, and C. Stoughton. *Data Mining the SDSS Skyscraper Database*. Technical report. Microsoft Research, 2002.
- [16] A. Guttman. R-Trees: A Dynamic Index Structure for Spatial Searching. *ACM SIGMOD*, pages 47–57, 1984.
- [17] D. Hilbert. Über die stetige Abbildung einer Linie auf Flächenstück. *Math. Ann.*, **38**:459–460, 1891.
- [18] H. V. Jagadish, L. V. S. Lakshmanan, and D. Srivastava. Snakes and sandwiches: optimal clustering strategies for a data warehouse. *SIGMOD Rec.*, **28**(2):37–48. ACM Press, 1999.
- [19] N. Koudas, C. Faloutsos, and I. Kamel. Declustering Spatial Databases on a Multi-Computer Architecture. *International Conference on Extending Database Technology* (Avignon, France), 1996.
- [20] B. Moon, H. V. Jagadish, C. Faloutsos, and J. H. Saltz. *Analysis of the clustering properties of Hilbert space-filling curve*. Technical report. University of Maryland at College Park, 1996.
- [21] Office of Science Data-Management Workshops. *The Office of Science Data-Management Challenge*. Technical report. Department of Energy, 2005.
- [22] J. A. Orenstein. Spatial query processing in an object-oriented database system. *ACM SIGMOD*, pages 326–336. ACM Press, 1986.
- [23] S. Prabhakar, K. Abdel-Ghaffar, D. Agrawal, and A. E. Abbadi. Efficient Retrieval of Multidimensional Datasets through Parallel I/O. *International Conference on High Performance Computing*, page 375. IEEE Computer Society, 1998.
- [24] C. Ruemmler and J. Wilkes. An introduction to disk drive modeling. *IEEE Computer*, **27**(3):17–28, March 1994.
- [25] J. Schindler and G. R. Ganger. *Automated disk drive characterization*. Technical report CMU-CS-99-176. Carnegie-Mellon University, Pittsburgh, PA, December 1999.
- [26] J. Schindler, J. L. Griffin, C. R. Lumb, and G. R. Ganger. Track-aligned extents: matching access patterns to disk drive characteristics. *Conference on File and Storage Technologies* (Monterey, CA, 28–30 January 2002), pages 259–274. USENIX Association, 2002.
- [27] J. Schindler, S. W. Schlosser, M. Shao, A. Ailamaki, and G. R. Ganger. Atropos: a disk array volume manager for orchestrated use of disks. *Conference on File and Storage Technologies* (San Francisco, CA, 31 March–02 April 2004). USENIX Association, 2004.
- [28] S. W. Schlosser, J. Schindler, A. Ailamaki, and G. R. Ganger. *Exposing and exploiting internal parallelism in MEMS-based storage*. Technical Report CMU-CS-03-125. Carnegie-Mellon University, Pittsburgh, PA, March 2003.
- [29] M. Seltzer, P. Chen, and J. Ousterhout. Disk scheduling revisited. *Winter USENIX Technical Conference* (Washington, DC, 22–26 January 1990), pages 313–323, 1990.
- [30] M. Shao, J. Schindler, S. W. Schlosser, A. Ailamaki, and G. R. Ganger. Clotho: Decoupling memory page layout from storage organization. *International Conference on Very Large Databases* (Toronto, Canada, 31 August–2 September 2004), 2004.
- [31] M. Shao, S. W. Schlosser, S. Papadomanolakis, J. Schindler, A. Ailamaki, C. Faloutsos, and G. R. Ganger. *MultiMap: Preserving disk locality for multidimensional datasets*. Carnegie Mellon University Parallel Data Lab Technical Report CMU-PDL-05-102. March 2005.
- [32] A. Shukla, P. Deshpande, J. F. Naughton, and K. Ramasamy. Storage Estimation for Multidimensional Aggregates in the Presence of Hierarchies. *International Conference on Very Large Databases*, pages 522–531. Morgan Kaufmann Publishers Inc., 1996.
- [33] K. Stockinger, D. Dullmann, W. Hoschek, and E. Schikuta. Improving the Performance of High-Energy Physics Analysis through Bitmap Indices. *Database and Expert Systems Applications*, pages 835–845, 2000.
- [34] T. Stoehr, H. Maertens, and E. Rahm. Multi-Dimensional Database Allocation for Parallel Data Warehouses. *International Conference on Very Large Databases*, pages 273–284. Morgan Kaufmann Publishers Inc., 2000.
- [35] N. Talagala, R. H. Arpaci-Dusseau, and D. Patterson. *Microbenchmark-based extraction of local and global disk characteristics*. Technical report CSD-99-1063. University of California at Berkeley, 13 June 2000.
- [36] B. L. Worthington, G. R. Ganger, and Y. N. Patt. Scheduling algorithms for modern disk drives. *ACM SIGMETRICS Conference on Measurement and Modeling of Computer Systems* (Nashville, TN, 16–20 May 1994), pages 241–251. ACM Press, 1994.
- [37] B. L. Worthington, G. R. Ganger, Y. N. Patt, and J. Wilkes. Online extraction of SCSI disk drive parameters. *ACM SIGMETRICS Conference on Measurement and Modeling of Computer Systems* (Ottawa, Canada), pages 146–156, May 1995.
- [38] H. Yu, D. Agrawal, and A. E. Abbadi. Tabular placement of relational data on MEMS-based storage devices. *International Conference on Very Large Databases* (Berlin, Germany, 09–12 September 2003), pages 680–693, 2003.
- [39] H. Yu, K.-L. Ma, and J. Welling. Automated Design of Multidimensional Clustering Tables for Relational Databases. *International Conference on Very Large Databases*, 2004.
- [40] H. Yu, K.-L. Ma, and J. Welling. A Parallel Visualization Pipeline for Terascale Earthquake Simulations. *ACM/IEEE conference on Supercomputing*, page 49, 2004.
- [41] Y. Zhao, P. M. Deshpande, and J. F. Naughton. An array-based algorithm for simultaneous multidimensional aggregates. *ACM SIGMOD International Conference on Management of Data* (Tucson, AZ, 13–15 May 1997). Published as *SIGMOD Record*, **26**(2):159–170. ACM, 1997.